

Reduction Behaviour of Electric Arc Furnace Dust (EAFD)-Coal Composite Pellet in a Muffle Furnace

Banty Kumar¹ · Gour Gopal Roy¹

Received: 7 March 2023 / Accepted: 1 May 2023 / Published online: 18 May 2023
© The Institution of Engineers (India) 2023

Abstract This investigation reports the effect of various operating parameters like amount of carbon, holding time, and heating rate on the nugget formation of EAFD (electric arc furnace dust)-coal composite pellets in muffle furnace at 1200 °C, the lowest Temperature reported. At moderate pellet heating rate (furnace heating rate at 25 °C/min), a unique coconut shell-iron nugget formed, with slag at the shell, DRI at the center, and iron nugget in the annular space, the thickness of which increased with the holding time. At a much higher heating rate under flash heating, nugget formation could not be achieved as the pellet exploded under internal gas pressure. XRD and SEM/EDS analysis characterized the obtained nuggets and slag and Factsage 6.4 was used to calculate thermodynamics stable phases.

Keywords EAF dust · Heating rate · Iron nugget · Composite pellets

Introduction

In 2021, world's crude steel production reached 1950 million tonnes [1]. The production of crude steel generates significant quantities of solid waste (iron bearing dust, sludge, and slag), forming a secondary sources of iron, which is also an environmental hazard [2–4]. Steel plant dust is a valuable by product of the steel manufacturing industry, taking account for about 10% of overall production of crude steel [5].

Electric arc furnaces (EAF) are a popular alternative to the traditional basic oxygen furnace (BOF) manufacturing process for carbon and alloy steels. EAF produces approximately 30% of crude steel by melting scrap [6]. Several authors have reported dust formation during EAF operations [7, 8]. EAFD is reported to form due to explosion of CO bubbles at the slag-gas interface and surface liquid turbulence [9]. Furthermore, volatile elements are present in the dust as oxide particulates. Fine dust particles travel out with gas stream and accumulated by de-dusting devices. In a typical EAF process, electric arc furnace dust (EAFD) produces about 1–2% of the charge [10, 11]. The worldwide EAF dust emission in 2014 increased to 8.764 million tonnes.

The composition of the EAFD depends on the quality of scrap, liquid iron and DRI used. The most abundant elements present in the EAFD are iron, zinc, and calcium, and the zinc content may vary up to 35%, while the iron in the range of 25–50%. Since EAFD contains heavy metals like lead, chromium, and cadmium, it is classified as toxic waste material by many countries [12]. This arrangement implies dust cannot be discarded in any conventional landfill site. As a result, the recovery of these resources is critical to environmental protection. Waelz kiln, Rotary Hearth Furnace (RHF), PRIMUS, OXYCUP, OXYFINES, and Ausmelt are some of the commercial processes where EAFD has been treated. The Waelz kiln, RHF, and the OxyCup are currently the primary methods for treating EAFD [13]. Although these processes can recycle iron and steel industry's dust and sludge, they all possess some demerits. For instance, the Waelz kiln requires more raw materials, consumes more energy, has unsteady production and operation, and with a limited capacity [14]. Metalized pellets are the RHF's main product, but they have a high sulphur content, and the process is inefficient and costly [15]. The OxyCup process produces molten iron and has relatively broad raw

✉ Banty Kumar
bantyl15@gmail.com

¹ Department of Metallurgical & Materials Engineering,
Indian Institute of Technology, Kharagpur 721302, WB,
India

material requirements. However, its maintenance is difficult with short operation cycle [10].

There are very limited articles that have been reported on the reduction behaviour of EAF dust. Most of them are on the recovery of Zinc. The current study aims to recover iron nuggets from EAFD at a comparatively lower temperature. The effect of carbon content, reduction time, and heating rate on iron yield and nugget formation has been studied.

Experimental Details

Raw Materials

This study’s raw materials are EAF dust, with total iron content Fe(t), as 48%, coal fines with 63% fixed carbon (FC), and bentonite as a binder. The bentonite used as the binder is of commercial grade with 5–10% loss on drying at 105 °C. The EAFD contained 5.97% Loss on Ignition (LOI), and coal contained 26.9% volatile matter (VM), respectively. The chemical composition of EAF dust, bentonite, and coal ash, used in the present study, is determined by XRF (Model: BRUKER-S8 TIGER) and is presented in Table 1.

The results of XRD analysis of the EAF dust is shown in Fig. 1. Iron appears as magnetite (Fe₃O₄), hematite (Fe₂O₃), franklinite (Fe₂O₄Zn), and Bixbyite (FeMnO₃). Magnetite and zinc ferrite are the most common forms.

The distribution of particle size of EAFD, Bentonite and Coal has been estimated following the standard test method for Sieve Analysis (ASTM-B214) and presented in Table 2. The majority of the EAF dust (38 wt.%) lie between the size of 150 to 105µm. Similarly, the majority of bentonite (36

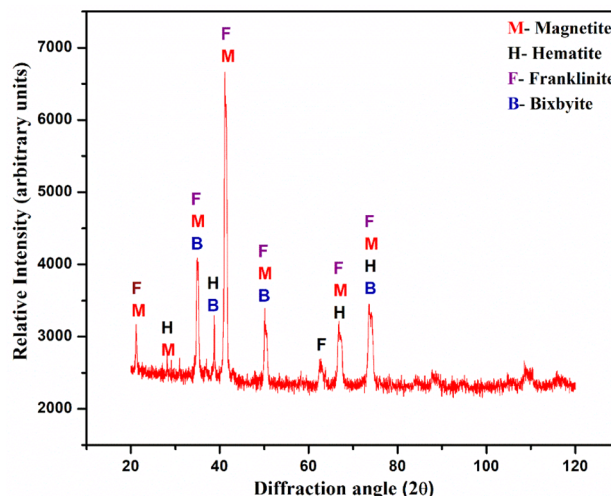


Fig. 1 The XRD analysis of the EAF dust

wt.%) lies between 74 to 53 µm, and in coal, 43 wt.% of lies between 105 to 74 µm.

Procedure

The EAF dust and coal powder were mixed with three wt.% bentonite. The mixing was done using a rotating glass bottle for 8–10 h. Pellet of different carbon to oxygen atomic ratios (representing the atomic ratio of carbon to oxygen in the pellet mix; carbon originating from fixed carbon of coal and oxygen from iron oxide in pellet mix) 1, 1.2, 1.5, and 2 were made. Pellets were made manually by mixing the powder with optimum distilled water. The green pellets were air-dried for 48 h before being furnace dried at 200 °C for two hours to remove physical moisture. The weight of the pellets was determined after drying.

The pellet is loaded into the muffle furnace in an alumina crucible for reduction. A lid was used in the crucible to restrict the re-oxidation of metallic iron. For the base case, the reduction was carried out at 1200 °C for 20 min of holding time with a heating rate of 25 °C/min. Experiments are carried out in two heating rates. In Case 1, pellets are kept in the furnace from the onset of heating, where the pellets can

Table 1 Chemical composition of composite pellet materials

Analyte/Wt.%	EAF Dust	Bentonite	Coal
Fe(t)	48.07	6.685	0.22
MnO	6.7	–	–
CaO	3.85	0.93	0.18
SiO ₂	3.79	58.3	6.30
MgO	2.33	2.05	0.02
SO ₃	2.13	–	0.08
ZnO	2.08	–	–
K ₂ O	1.8	1.07	0.06
Na ₂ O	1.43	5.89	–
Al ₂ O ₃	0.48	17.47	1.62
P ₂ O ₅	0.41	–	0.15
Cr ₂ O ₃	0.35	–	–
PbO	0.27	–	–
TiO ₂	–	1.81	0.11
LOI/VM	5.97	–	26.9
FC	–	–	63.38

Table 2 EAF dust, coal, and bentonite particle size distribution

Size Range/µm	EAF Dust	Bentonite	Coal
+ 150	15.32	3.01	10.58
– 150 + 105	37.90	14.21	32.68
– 105 + 74	22.53	17.00	43.34
– 74 + 53	18.77	36.15	12.5
– 53 + 44	4.22	11.18	0.9
– 44	1.22	17.88	–

attain a maximum heating rate equal to the furnace heating rate initially. In case 2, flash heating is used where the pellets are kept in the furnace when the furnace attains the desired temperature, 1200 °C. Under flash heating, as the pellets are exposed to a high temperature from the beginning, the pellet attains a heating rate much higher than the standard heating rate of the furnace.

The phase analysis of the reduced products, nugget, slags and powder layers, was performed on RIGAKU MINIFLEX 600 x-Ray diffractometer. Cobalt (K_{α} 1.79 Å) target with iron beta filter has been used with the step size of 0.02 degree and speed of 10 degrees per minute. The qualitative phase analysis has been done by using X'Pert HighScore software. SEM/EDS study was performed on a TESCAN MIRA3, SEM/EDS machine. An Energy Dispersive X-Ray Analyser (EDS) is also used to provide elemental identification and quantitative compositional information at different points.

Results and Discussion

Effect of Coal Amount

Figure 2 depicts a cross-sectional view of dissected reduced pellets at various C/O ratios. The reduction was done at 1200 °C with a normal heating rate of 25 °C/min for 20 min of holding time. As shown in Fig. 2a, three distinct layers are observed at a C/O molar ratio of 1. On the surface, there is a slag layer followed by an iron layer and, finally, a powdery core. At comparatively higher carbon level, C/O = 1.2, the thickness of the iron layer decreases. With a further increase in carbon level, C/O = 1.5, the outer slag layer vanished, iron layer thickness further decreased, and a powdery core expanded. With extreme carbon, C/O = 2.0, no iron layer was visible.

Based on factsage (Factsage 6.4) calculation, it was observed that at C/O = 1, slag remains in a liquid state (77% liquid), and iron remains in a solid state. Therefore, slag oozes out of the solid iron layer and accumulates at the surface. At the core, heating is not sufficient to melt the slag for its separation. As the carbon level increases in the pellet, the Factsage calculation shows the formation of liquid iron that makes the iron layer more consolidated, reducing its thickness. High carbon may also restrict heat transfer to the core, limiting the liquid iron formation. Figure 3 shows the XRD result of three layers formed, as shown in Fig. 2a. On the surface, various slag constituents are observed mixed with some amount of iron oxides. In the iron layer, iron is the predominant phase. In the powdery core layer also, the predominant phase is iron mixed with some slag constituents. In the iron layer, temperature was sufficient to melt the carburized iron, which subsequently coalesced to form a consolidated iron layer. In the core, due to insufficient heat penetration, the reduced iron could not melt, coalesce, and remains mixed with slag constituents.

Effect of Heating Rate

Figure 4 depicts the remains of the reduced pellets after flash heating at 1200 °C composite pellet with a C/O ratio of 1. It is seen that the reduced pellets have exploded, which contained several iron particles along with powdery slag constituents. In flash heating, a dried green ball was introduced into the muffle furnace when the furnace attained 1200 °C. Since the pellet is exposed to a high temperature from the beginning, it sets a very high pellet heating rate. Release of volatile, LOI, reduction gases, localized liquid formation due to gangue of coal ash and EAFD, and closures of pores in conjunction with a high heating rate that initiates all processes at a faster rate builds up internal pressure, leading to rupture of pellet. When EAFD-coal composite pellets were reduced with

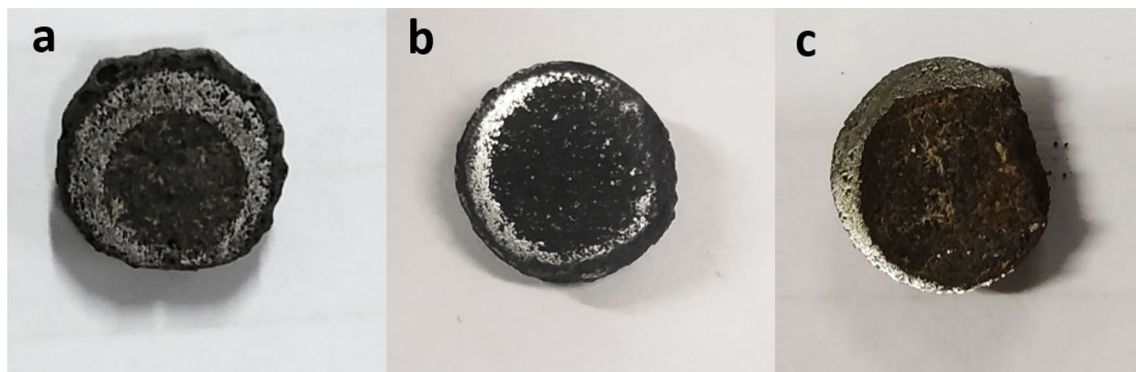


Fig. 2 Effect of coal amount on reduction behaviour in composite pellet C/O molar ratio of (a) 1 (b) 1.2 (c) 1.5 at 1200 °C with heating rate of 25 °C/min and 20 min holding time

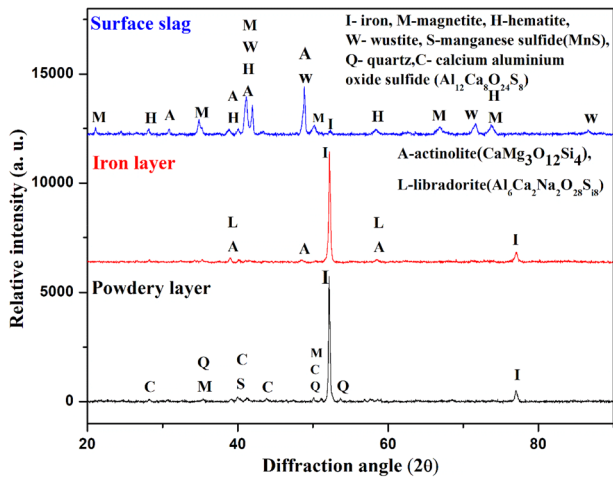


Fig. 3 XRD result of three layer formed by reduction of composite pellet containing C/O-1, at 1200 °C for 20 min with the heating rate of 25 °C/min



Fig. 4 EAFD – coal composite pellet, containing C/O molar ratio of 1, reduced at 1200°C under flash heating

a normal furnace heating rate of 25 °C/min at 1200 °C (when pellets are put into the furnace at the onset of furnace heating), a three layers cross section of dissected reduced pellet is observed (Fig. 2a).

Effect of Holding Time

Figure 5 shows a photograph of the cross-section of the dissected reduced pellet (C/O = 1) at 1200 °C with an increase in holding time with a furnace heating rate of 25 °C/min. It is observed that with an increase in holding time, the iron layer thickness increases progressively and penetrates toward the core.

SEM Results Analysis

Figure 6a shows the SEM image of the reduced composite pellet near the edge with C/O = 1 for 6 min of holding at 1200 °C. Figure 6b shows the magnified image of the iron layer. It is seen that slag (grey region) is entrapped into the iron particles (white region). It is consistent with our factage calculation that at C/O = 1, the iron remains solid and slag in the liquid state at 1200 °C. Thus slag wets the iron particles making a morphology as shown in Fig. 6b. The black particle, Fig. 6 spot 2, is $\text{SiO}_2 \cdot \text{Al}_2\text{O}_3 \cdot \text{Na}_2\text{O} \cdot \text{K}_2\text{O}$. It is the initial gangue particle of the EAFD. At high temperature, SiO_2 starts reacting with the present basic oxide, and forms new phase (Fig. 6, spot 4), $\text{SiO}_2 \cdot \text{CaO} \cdot \text{MgO} \cdot \text{MnO}$. It grows through the surface of the other particles.

Figure 7 shows the SEM image of the center of the reduced pellet for 6 min of holding at 1200 °C. It is observed that the core contains some reduced and unreduced iron (see EDS result). Reduced iron is in small particle form. They could not melt and coalesce due to a lack of temperature.

Figure 8 shows the elemental mapping of the iron layer of the pellet for 20 min holding time of composite pellet containing C/O-1 at 1200 °C with a heating rate of 25 °C/min. From iron mapping, it is evident that iron was melted and coalesced. Some slag phases are also remaining entrapped in the iron.

Figure 9 shows the SEM image of the outer slag layer of the reduced pellet (C/O = 1) at 1200 °C for 20 min of holding time. The slag layer is found to consist of three phases. Spot 2 results show $\text{SiO}_2 \cdot \text{CaO} \cdot \text{MgO} \cdot \text{MnO}$. The black particle, spot 3, is $\text{SiO}_2 \cdot \text{Al}_2\text{O}_3 \cdot \text{Na}_2\text{O} \cdot \text{K}_2\text{O}$. Iron is present in FeO form (spot 1), which is also obtained in the XRD result (Fig. 3).

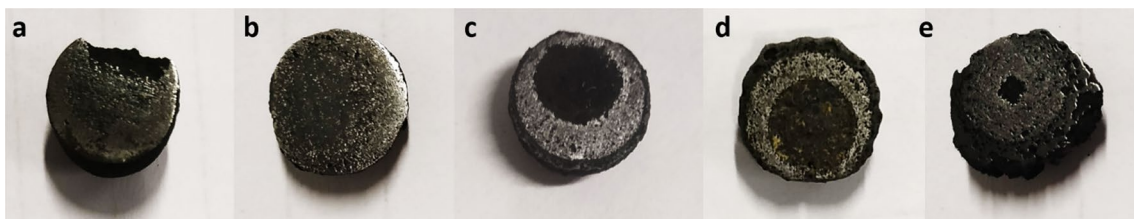


Fig. 5 Photographs of different holding time (a) 3 min (b) 6 min (c) 10 min (d) 20 min (e) 60 min on composite pellet containing C/O molar ratio 1 at 1200 °C with heating rate of 25 °C/min

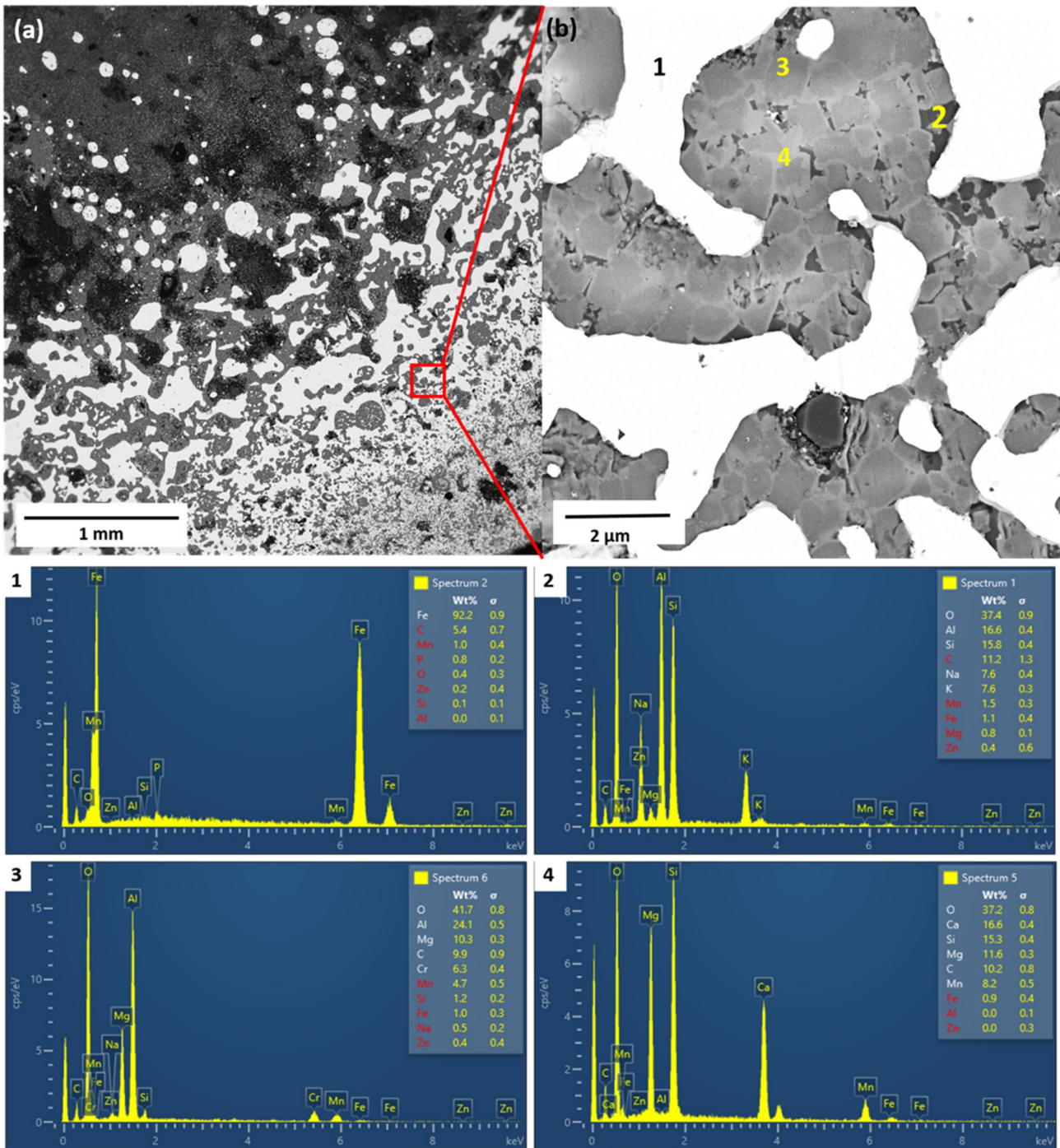


Fig. 6 SEM image and EDS of iron layer of the reduced pellet for 6 min of holding time of the composite pellet containing C/O=1 at 1200 °C with heating rate of 25 °C/min

Conclusions

- EAFD-coal composite pellet was successfully reduced in a muffle furnace at 1200 °C with a heating rate of 25 °C/min. A composite pellet containing C/O = 1 forms three

layers. There was a slag layer on the surface, followed by a middle iron layer, and finally, a powdery core layer consisting of solid iron particles mixed with gangue substances.

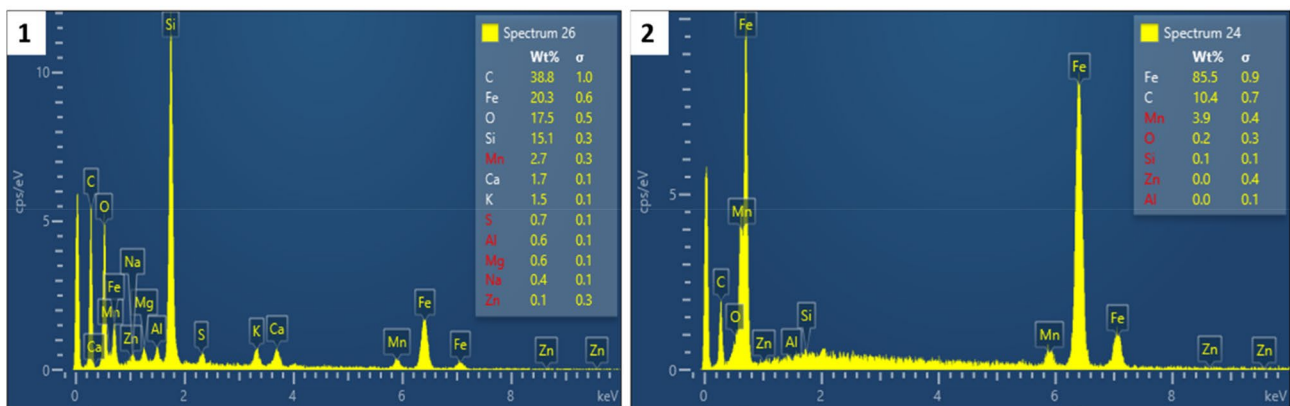
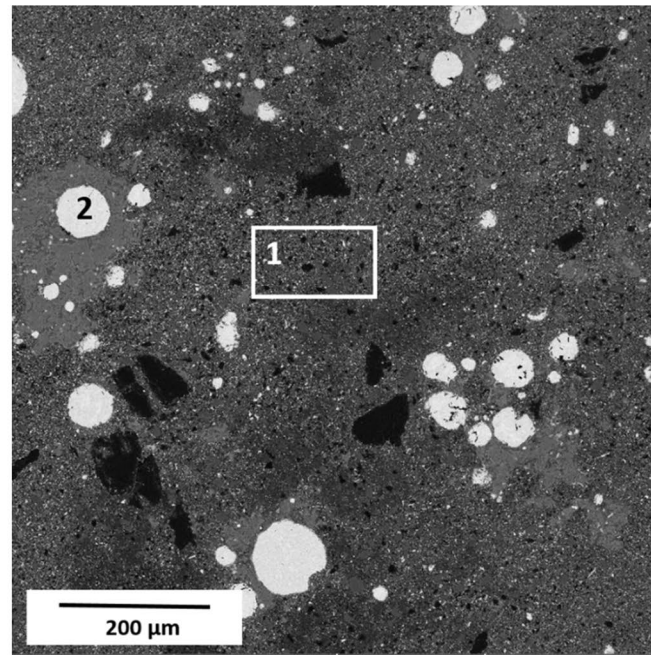


Fig. 7 SEM image of the center of reduced pellet for 6 min of holding time of the composite pellet containing C/O-1 at 1200 °C with heating rate of 25 °C/min

- With an increase in carbon in the pellet, the surface slag layer vanished and the iron layer consolidated and reduced in thickness.
- With an increase in holding time, the iron layer expands with a corresponding decrease in the powdery core thickness. At 60 min of holding time for a reduced pellet with C/O = 1, the iron layer moved to the center.
- Due to high volatile matter in coal and LOI in EAFD, flash heating (representing a high heating rate) exploded the pellet into small pieces.
- The optimum conditions for nugget formation were identified as one hour holding at 1200 °C at C/O ratio of 1.

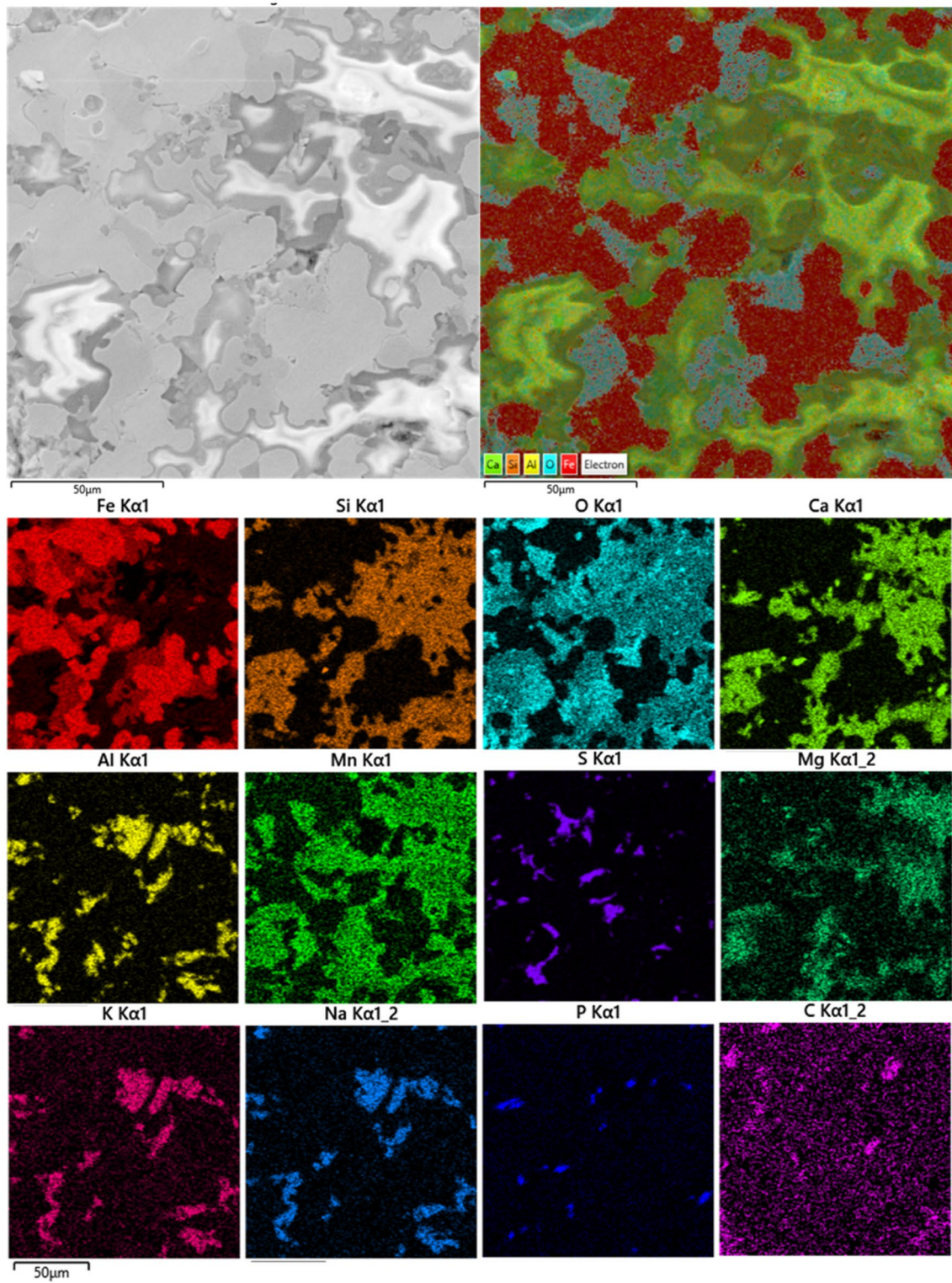


Fig. 8 Elemental mapping of the iron layer of the pellet for 20 min holding time of composite pellet containing $C/O=1$ at $1200\text{ }^{\circ}\text{C}$ with heating rate of $25\text{ }^{\circ}\text{C}/\text{min}$

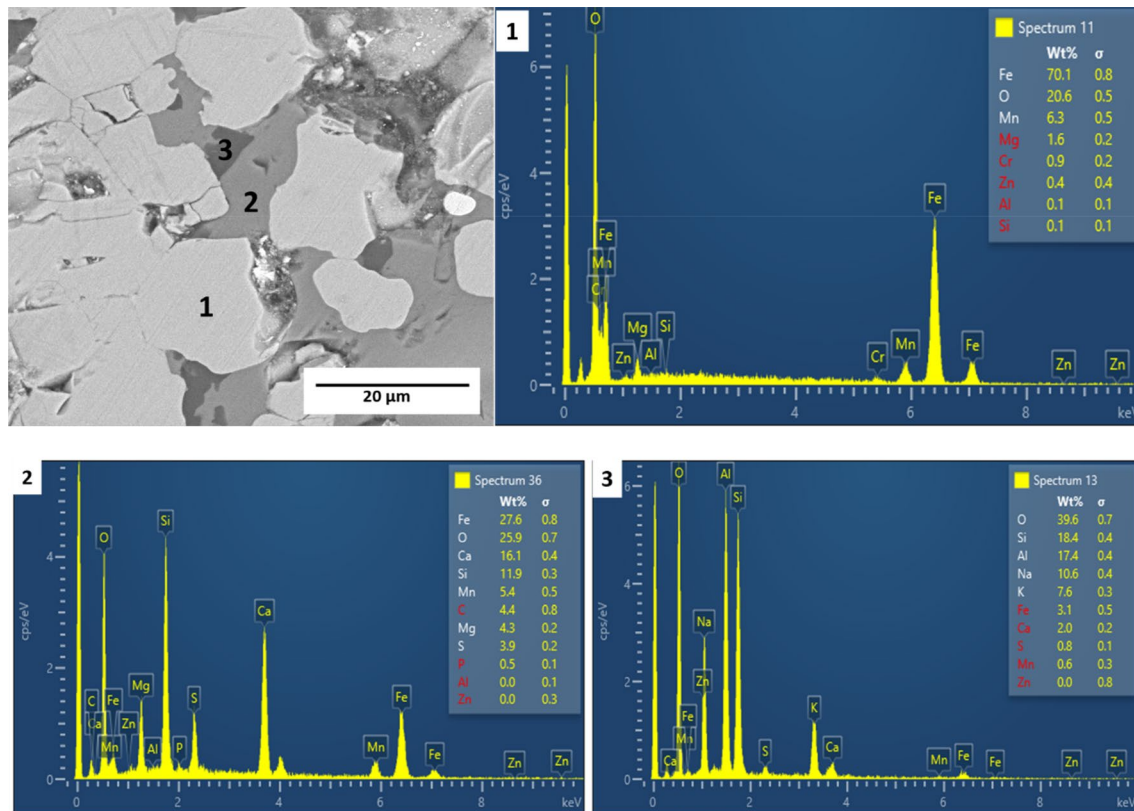


Fig. 9 SEM image and EDS of the slag layer of the reduced pellet for 20 min holding time of the composite pellet containing C/O-1 at 1200 °C with heating rate of 25 °C/min

Funding The authors declare that no funds, grants, or other forms of support were received during the preparation of this manuscript.

Declarations

Conflict of interest On behalf of all authors, the corresponding author states that there is no conflict of interest.

References

- World Steel Association, 2022; <https://worldsteel.org/media-center/press-releases/2022/world-steel-in-figures-2022-now-available/>
- K.H. Mo, U.J. Alengaram, M.Z. Jumaat, S.P. Yap, Feasibility study of high volume slag as cement replacement for sustainable structural lightweight oil palm shell concrete. *J. Clean. Prod.* **91**, 297–304 (2015)
- H.I. Gomes, W.M. Mayes, M. Rogerson, D.I. Stewart, I.T. Burke, Alkaline residues and the environment: a review of impacts, management practices and opportunities. *J. Clean. Prod.* **112**, 3571–3582 (2016)
- H. Pan, X. Zhang, J. Wu, Y. Zhang, L. Lin, G. Yang, S. Deng, L. Li, X. Yu, H. Qi, H. Peng, Sustainability evaluation of a steel production system in China based on energy. *J. Clean. Prod.* **112**(2), 1498–1509 (2016)
- J.B. Dutra, P.R.P. Paiva, L.M. Tavares, Alkaline leaching of zinc from electric arc furnace steel dust. *Min. Eng.* **19**(5), 478–485 (2006)
- World steel Association, 2019. World Steel Association, Steel Statistical Yearbook 2019; Available on Internet: <http://www.worldsteel.org/statistics/statistics-archive/yearbook-archive.html>.
- J.P. Morris, J.P. Riott, E.G. Illig, A new look at the cause of fuming. *JOM.* **18**(7), 803–8101 (1966)
- A.F. Ellis, J. Glover, Mechanism of fume formation in oxygen steelmaking. *J. Iron Steel Inst.* **209**, 593–599 (1971)
- A.G. Guézennec, J.C. Huber, F. Patisson, Ph. Sessiecq, J.P. Birat, D. Ablitzer, Dust formation by bubble-burst phenomenon at the surface of a liquid steel bath. *ISIJ Int.* **44**, 1328–1333 (2014)
- X. Lin, Z. Peng, J. Yan, Z. Li, J.Y. Hwang, Y. Zhang, G. Li, T. Jiang, Pyrometallurgical recycling of electric arc furnace dust. *J. Clean. Prod.* **149**, 1079–1100 (2017)
- A. Loaiza, S. Cifuentes, H.A. Colorado, Asphalt modified with superfine electric arc furnace steel dust (EAF dust) with high zinc oxide content. *Constr. Build. Mater.* **145**, 538–547 (2017)
- Environmental Protection Agency, 1991; <https://www.epa.gov/rcra/resource-conservation-and-recovery-act-rcra-regulation#haz>.
- T.K. Kumar, G.G. Roy, A review on processing of electric arc furnace dust (EAFD) by pyro-metallurgical processes. *Trans. Indian Inst. Met.* **75**(5), 1101–1112 (2022)
- J. Antrekowitsch, G. Rösler, S. Steinacker, State of the art in steel mill dust recycling. *Chem. Ing. Tech.* **87**, 498–1503 (2015)

15. T. Suetens, B. Klaasen, K. Van Acker, B. Blanpain, Comparison of electric arc furnace dust treatment technologies using exergy efficiency. *J. Clean. Prod.* **65**, 152–167 (2014)
16. M. Zhang, J. Li, Q. Zeng, Q. Mou, An experimental study on the reduction behavior of dust generated from electric Arc furnace. *J. Appl. Sci.* **9**, 3604–3614 (2019)

Springer Nature or its licensor (e.g. a society or other partner) holds exclusive rights to this article under a publishing agreement with the author(s) or other rightsholder(s); author self-archiving of the accepted manuscript version of this article is solely governed by the terms of such publishing agreement and applicable law.

Publisher's Note Springer Nature remains neutral with regard to jurisdictional claims in published maps and institutional affiliations.